Since January 2020 Elsevier has created a COVID-19 resource centre with free information in English and Mandarin on the novel coronavirus COVID-19. The COVID-19 resource centre is hosted on Elsevier Connect, the company's public news and information website.

International Journal of Infectious Diseases 109 (2021) 310–314

Contents lists available at ScienceDirect

International Journal of Infectious Diseases

journal homepage: www.elsevier.com/locate/ijid

Effectiveness of different types of mask in aerosol dispersion in SARS-CoV-2 infection

Gokhan Tanisali[a,b,*], Ahmet Sozak[c], Abdul Samet Bulut[c], Tolga Ziya Sander[c], Ozlem Dogan[d,h], Çağdaş Dağ[b,e,h], Mehmet Gönen[f,h], Fusun Can[d,h], Hasan DeMirci[b,g,h], Onder Ergonul[d,h]

[a] Department of Material Science and Engineering, Koç University, Istanbul, Turkey
[b] Department of Molecular Biology and Genetics, Koç University, Istanbul, Turkey
[c] Microelectronics, Guidance and Electro-Optics Business Sector, Optical and Optomechanical Design Department, Aselsan Inc., Ankara, Turkey
[d] School of Medicine, Department of Infectious Diseases and Clinical Microbiology, Koç University, Istanbul, Turkey
[e] Nanofabrication and Nanocharacterization Centre for Scientific and Technological Advanced Research, Koç University, Istanbul, Turkey
[f] Department of Industrial Engineering, College of Engineering, Koç University, Istanbul, Turkey
[g] Stanford PULSE Institute, SLAC National Laboratory, Menlo Park, CA, USA
[h] Koç University İşBank Centre for Infectious Diseases, Istanbul, Turkey

ARTICLE INFO

Article history:
Received 25 March 2021
Revised 10 June 2021
Accepted 12 June 2021

Keywords:
SARS-CoV-2
COVID-19
Mask types
Aerosol dispersion
Schlieren Imaging

ABSTRACT

Objective: To compare the effectiveness of different mask types in limiting the dispersal of coughed air.

Method: The Schlieren method with a single curved mirror was used in this study. Coughed air has a slightly higher temperature than ambient air, which generates a refractive index gradient. A curved mirror with a radius of curvature of 10 m and a diameter of 60 cm was used. The spread of the cough wavefront was investigated among five subjects wearing: (1) no mask; (2) a single surgical mask; (3) a double surgical mask; (4) a cloth mask; (5) a valveless N95 mask; and (6) a valved N95 mask.

Results: All mask types reduced the size of the contaminated region significantly. The percentage reduction in the cross-sectional area of the contaminated region for the same mask types on different subjects revealed by normalized data suggests that the fit of a mask plays an important role.

Conclusions: No significant difference in the spread of coughed air was found between the use of a single surgical mask or a double surgical mask. Cloth masks may be effective, depending on the quality of the cloth. Valved N95 masks exclusively protect the user. The fit of a mask is an important factor to minimize the contaminated region.

Introduction

Coronavirus disease 2019 (COVID-19) is an acute respiratory illness caused by severe acute respiratory syndrome coronavirus-2 (SARS-CoV-2). The World Health Organization declared a pandemic situation on 11 March 2020. The basic reproductive rate (R0) of SARS-CoV-2 has been determined as 2.5, which is higher than the R0 of influenza, SARS-CoV-1 and Middle East respiratory syndrome coronavirus (Petersen et al., 2020). One of the most effective ways to prevent the spread of SARS-CoV-2 is proper use of masks. Although extensive research has been undertaken into the use of various types of mask (Tang et al., 2009; Simha and Rao, 2020), to the authors' knowledge, there are no comprehensive studies about the use of double masks. As such, there is an urgent need to measure the dispersal of a cough when two surgical masks are worn together.

Coughed air has a higher temperature than ambient air, which generates a refractive index gradient. Schlieren's method is a useful tool to image transparent fluids that exhibit variations in refractive index across the imaged area. It has been used in different applications in many engineering fields, as well as in bi-

* Corresponding author. Department of Material Science and Engineering, Koç University, Rumelifeneri, Sarıyer Rumeli Feneri Yolu, 34450 Sarıyer/İstanbul, Turkey.
E-mail addresses: htanisali@ku.edu.tr (G. Tanisali), oergonul@ku.edu.tr (O. Ergonul).

https://doi.org/10.1016/j.ijid.2021.06.029

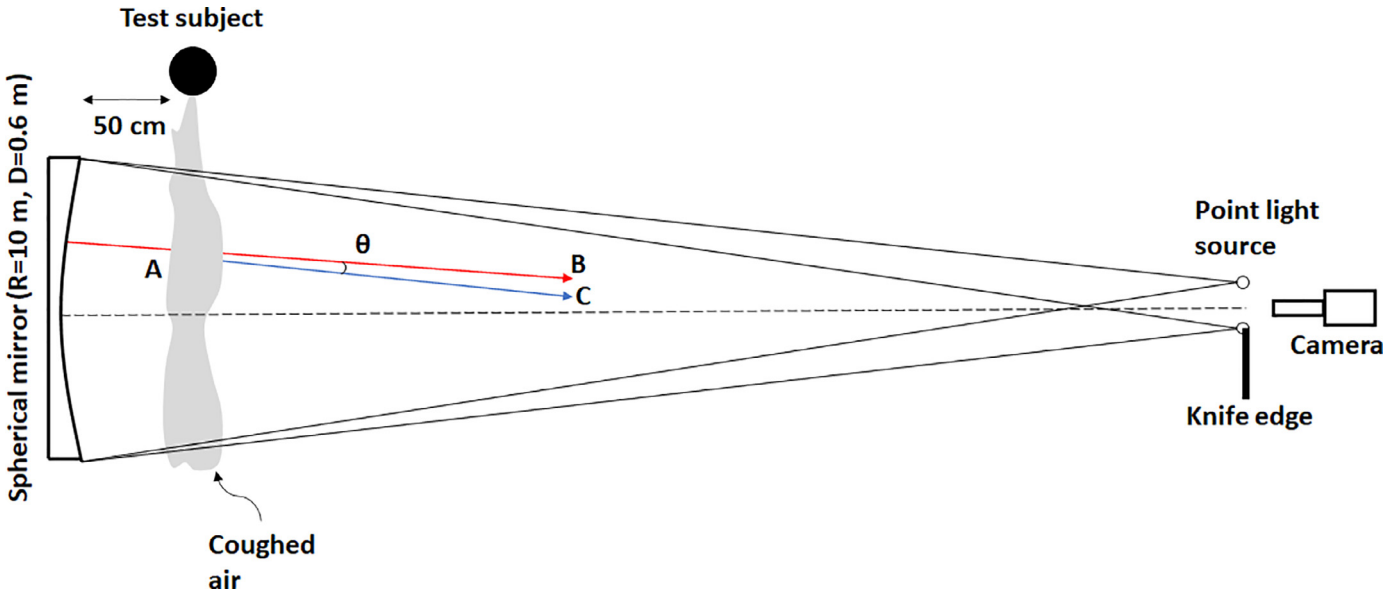

Figure 1. Schematic representation of the Schlieren set-up with a single curved mirror.

ology, including the investigation of flow visualization generated by insects (Liu et al., 2018), human thermal plume (Gena et al., 2020), protein crystal formation and hyperquenching protein crystals (Poodt et al., 2006, Warkentin and Thorne, 2007). The recent COVID-19 pandemic has turned research attention to transmission of respiratory diseases via droplets generated during coughing. Although studies have suggested slightly different droplet size distributions in coughed air, it can be safely said that the droplet sizes are of the order of microns. Previous work using a laser diffraction system (Zayas et al., 2012) or an aerodynamic particle sizer and scanning mobility particle sizer (Yang et al., 2007) reported that the majority of droplets produced are <5 μm in size. The use of face masks reduces the number of virus-laden droplets spread to the surrounding area; nevertheless, some droplets are still emitted through masks due to the small size of the droplets (Johnson et al., 2011; Asadi et al., 2020) or leaks due to improperly fitted masks. The risk of infection increases when coughed air travels greater distances. Schlieren imaging can help to determine the effectiveness of different mask types by employing refractive index variations in coughed air due to the temperature difference between exhaled and ambient air.

This study aimed to compare and measure the effectiveness of face masks in limiting the dispersal of coughed air using either single or double surgical masks (Mumu™, Istanbul, Turkey), valved and valveless N95 masks (3M™, Saint Paul, MN, USA), and cloth masks (from organically grown cotton). The outcome of this research did not consider the protection of the mask wearer but focused on the protection of others.

Materials and methods

Schlieren imaging

A schematic representation of Schlieren imaging can be seen in Figure 1. In the simple Schlieren set-up discussed here, a light source (either a point source or an extended source such as a slit) is placed slightly off-axis (a few centimetres), 2f away from the curved mirror where f is the focal length of the mirror. The light source is imaged next to itself, and a knife edge is placed close to the optical axis so that it blocks the desired portion of the incoming light. (Figure S1, see online supplementary material). The knife edge can move perpendicular to the optical axis so that it blocks the desired percentage of the incoming beam reaching the camera. When refractive index variations exist in the transparent medium between the light source and the curved mirror, the propagating beam experiences a slight change in its propagation direction in accordance with Snell's law (Figure S2, see online supplementary material). This is illustrated in Figure 1 as the beam (shown in red) entering the test area at point A would reach point B if there were no changes in the refractive index in the test area. However, slight variations in the refractive index induced by temperature changes bend the propagation direction of the beam by angle θ, and direct it to point C (deflected beam shown in blue). As a result, the incoming beam that would reach the camera is deflected down towards the knife edge and blocked by it (as illustrated in Figure 1), or the beam that would propagate towards the knife edge could have been deflected away from it and reached the camera. This, in turn, generates brighter and darker regions in the image, carrying information about the refractive index gradients in the test area.

A Schlieren set-up with a single curved mirror was assembled at Koç University Isbank Research Centre for Infectious Diseases, Istanbul, Turkey. A curved mirror with a radius of curvature of 10 m and a diameter of 60 cm was manufactured by Aselsan Inc. (Ankara, Turkey) for these experiments. The optomechanical design of the mirror used parametric optimization with finite element techniques for light weighting. The light weighting pattern of the back surface and flexure design at the mounting interface are crucial for the performance of a 60-cm-diameter mirror under gravity and mounting force to eliminate surface deformation. An aluminum alloy was chosen as the mirror material, and single point diamond turning was used as the manufacturing technique. The manufacturing process was developed specifically to obtain the required surface quality and precision because the required diameter of 60 cm is so close to the limit of a single point diamond turning machine (Figures S3 and S4, see online supplementary material). The feed rate and rotation speed of machining were optimized to improve surface irregularities and roughness.

A 21V, 150W fibre-optic illuminator (Bel Engineering SRL, Monza, Italy) was used with an attached optical aperture in front of it as a point light source. The light coming out of the aperture was imaged 3 cm away from itself, where a carpet blade was placed vertically as a knife edge to visualize horizontal refractive

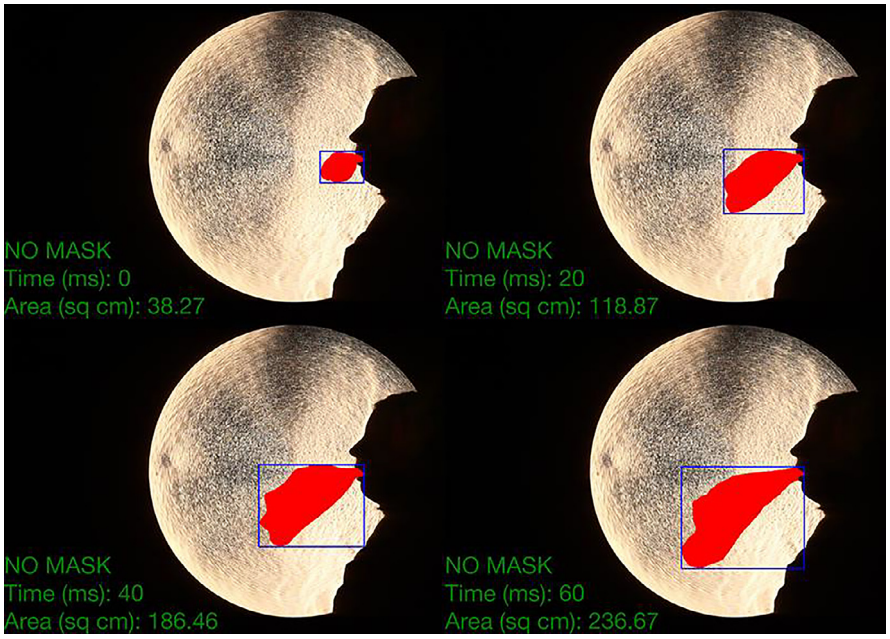

Figure 2. Propagation of the contaminated region for an unmasked case from initiation of the cough to 60 ms.

index variations in the test area due to warmer coughed air. Finally, the camera (EOS 800D; Canon Inc., Tokyo, Japan) was placed along the optical axis of the mirror, 5 cm behind the knife edge (Figure S1, see online supplementary material).

Mask experiments

Verbal consent of the test subjects were taken before starting the experiments. The test subjects were seated 50 cm in front of the mirror, next to the imaged area, facing perpendicular to the optical axis (Figure 1 and Figure S5, see online supplementary material). The field of view (60 cm), limited by the diameter of the mirror, was sufficient to investigate the propagation of the cough wavefront, defined as the interface between warmer coughed air and ambient air (Simha and Rao, 2020).

The contaminated region was defined as the region surrounded by the cough wavefront. Mask effectiveness was determined based on the size and shape of the contaminated region. Six different scenarios were studied to investigate the effectiveness of masks: (1) no mask, (2) a surgical mask, (3) a double surgical mask, (4) a cloth mask, (5) a valveless N95 mask, and (6) a valved N95 mask. For each scenario, five individual test subjects were initially instructed to cough while facing parallel to the mirror. They were advised to take a deep breath and cough at expiration. The exact distances changed +/- 5 cm during the experiments because the test subjects were not fully restrained when they produced voluntary coughs. The lower body of each test subject was covered with a nylon sheet as an insulator to minimize the interference of warm air dissipated by the test subject.

Results

Data analysis

The videos were recorded at 50 frames per second throughout the experiments. In each recording, the first frame was designated as the frame in which the cough was initiated. The cough wavefronts in the fourth frame, which corresponded to 60 ms after the initiation of the cough, were drawn manually as closed polygons. In each frame, in order to determine the area of the contaminated region, the area of the closed polygon was calculated. A frame with no obstacle in front of the mirror was used as the reference frame, in which the mirror was manually annotated as a closed polygon. Using the mirror dimensions, the areas calculated in other frames were converted into metric units. Propagation of the contaminated region for an unmasked case can be seen in Figure 2. Furthermore, contaminated regions 60 ms after initiation of the cough are shown in Figure 3 for each of the six cases for the same test subject. In the case of no mask, the mean cross-sectional contaminated region of the five subjects was 291 cm^2, representing – as expected – the largest contaminated area among all recorded scenarios (Figure 4a). The mean area was reduced to 61 cm^2, 67 cm^2 and 63 cm^2 when the subject's face was covered with a single mask, a double mask or a cloth mask, respectively. Valveless N95 masks showed the best performance, allowing a contaminated region of 52 cm^2 (Figure 4a). However, valved N95 masks were the least successful of all types of masks tested, with a contaminated region of 113 cm^2 (as seen in Figure 4a). To compare the percentage reduction in the contaminated region with different mask types, the areas were normalized by dividing them by the area of the unmasked case for each individual, respectively (see Figure 4b). The variance in the normalized values was, among other factors, due to the improper fitting of the masks for some of the test subjects (see Figure 4b). This can also be seen in Figure 3b–d, where there was leakage of coughed air above the nose.

Discussion

As the new SARS-CoV-2 variants emerged, extra precautions were taken, including the use of double masks as standard in many countries. However, this study found similar results for exhalational spread for single and double surgical masks. Cloth masks can be effective, depending on the quality of the cloth. The wavefront measurements confirmed that valved N95 masks exclusively protect the user. Mask fit is an important factor to minimize the contaminated region.

The majority of mask types were fairly successful in preventing the spread of the contaminated region by approximately 80%, while this prevention was approximately 60% for valved N95 masks (Figure 4b). This result was expected as valved N95 masks

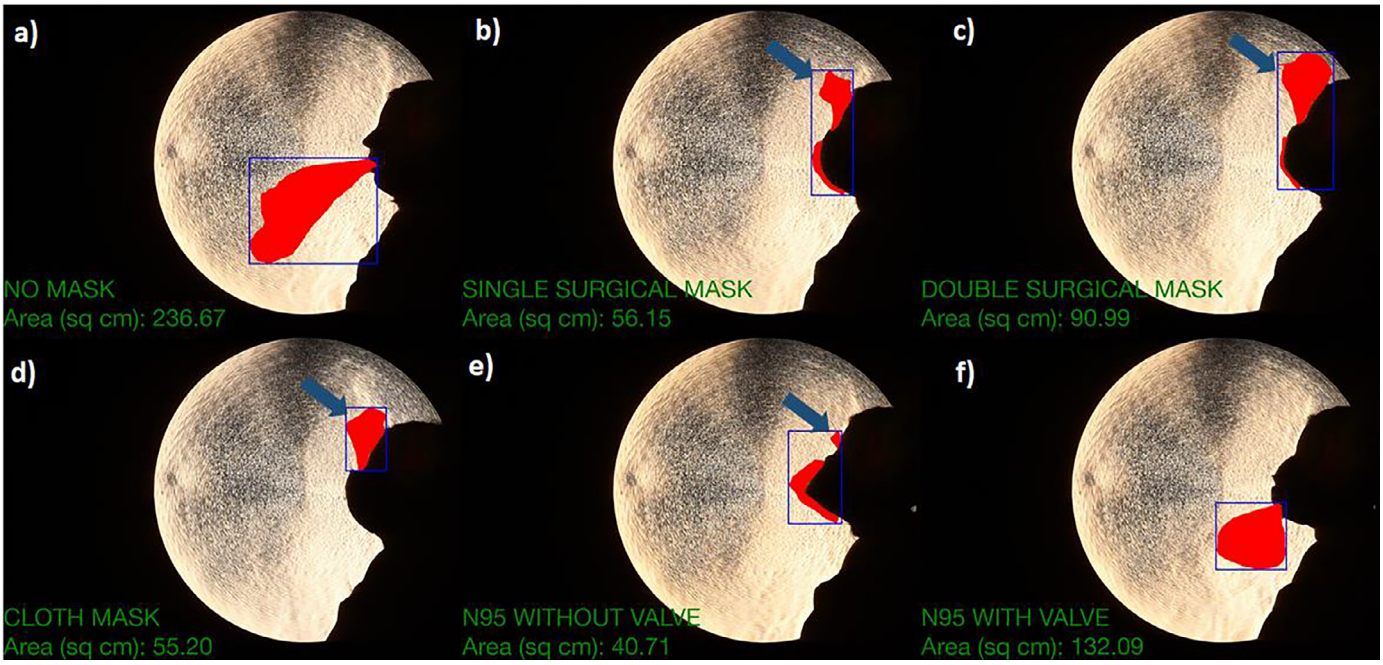

Figure 3. Contaminated regions at 60 ms after initiation of the cough for cases wearing: (a) no mask, (b) a surgical mask, (c) a double surgical mask, (d) a cloth mask, (e) a valveless N95 mask, and (f) a valved N95 mask. Note the leakage of air above the nose indicated by arrows.

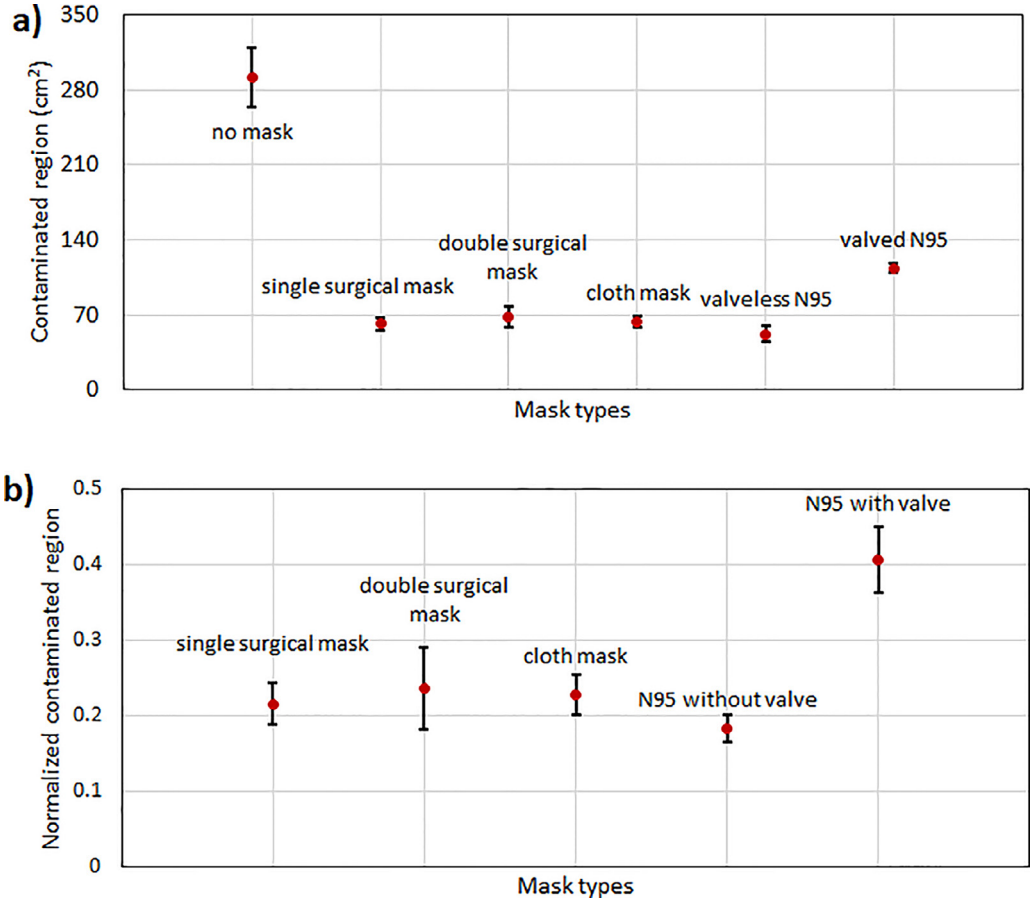

Figure 4. (a). Mean cross-sectional area of contaminated regions 60 ms after initiation of the cough. (b) Mean normalized cross-sectional area of contaminated regions for different mask types with respect to the unmasked case.

permit leakage of air through the valves. In this study, leakage was observed along the direction of the valves (Figure S6, see online supplementary material). This finding regarding valved N95 masks agrees with the results of previous studies (Staymates, 2020). Therefore, discouragement of the use of valved N95 masks in public places is appropriate. Instead, the use of valveless N95 masks should be preferred as they exhibit protection against inhalational exposure to viruses, and they were fairly successful in minimizing the contaminated region (Figure 3e and Figure 4). Another important point is that single and double surgical masks performed similarly in reducing the area of the contaminated region (Figure 3b,c and Figure 4). Although most of the coughed air escaped through the gap around the nose in Fig. 3b, this was not the case for all test subjects (Figure S7, see online supplementary material). A plausible explanation is that differences in the fit of the masks among different test subjects become more pronounced in double masking. As a result, this directs more coughed air above the nose in some test subjects, as in Figure 3b. The larger variation in double masking in Figure 4b also supports differences in mask fit between test subjects. The main limitation of this study is that the Schlieren technique only images warmer coughed air, and does not image individual aerosols or droplets. Therefore, although the dispersal of coughed air was fairly similar for single and double surgical masks, there may be differences between them in terms of the number of virus-laden particles emitted and their success in preventing inhalational exposure to viruses (Konda et al., 2020; Brooks et al., 2021). Furthermore, the concentration of droplets can be expected to be higher in air that is leaked through gaps (shown by the arrow in Figure 3b–e) as opposed to air that is leaked through the face mask as the former is not filtered. The effectiveness of cloth masks in reducing the contaminated region is also noteworthy.

Schlieren imaging is a very robust method and allows direct testing of real-life scenarios. These data suggest that people must wear masks appropriately, which means a mask conforms to the person's face at the nose, under the chin and on the cheeks rather than gaping and letting air in. Although double layering adds extra filtration, most of the benefit comes in ensuring that gaps around the mask are covered, because all masks do not fit equally. Although double surgical masks are recommended in many countries, the increased emphasis should be on 'better masking' and better mask use, as the next phase of the pandemic may well be dominated by the fight against emerging respiratory pathogens.

Declaration of Competing Interest

None declared.

Acknowledgements

The authors gratefully acknowledge use of the services and facilities at Koç University Isbank Research Centre for Infectious Diseases. HD acknowledges support from National Science Foundation (NSF) Science and Technology Centers Grant NSF-1231306 (Biology with X-ray Lasers, BioXFEL).

Funding

This publication was supported by the 2232 International Fellowship for Outstanding Researchers Program of TÜBİTAK (Project No: 118C270). However, responsibility for the publication lies with the authors. The financial support from TÜBİTAK does not mean that the content of the publication is approved in a scientific sense by TÜBİTAK. CD acknowledges support from TÜBİTAK (Project No: 120Z594).

Ethical approval

This study was approved by Koç University Institutional Review Board (2021.255.IRB1.087).

Supplementary materials

Supplementary material associated with this article can be found, in the online version, at doi:10.1016/j.ijid.2021.06.029.

References

Asadi S, Cappa CD, Barreda S, Wexler AS, Bouvier NM, Ristenpart WD. Efficacy of masks and face coverings in controlling outward aerosol particle emission from expiratory activities. Sci Rep 2020;10:15665.
Brooks JT, Beezhold DH, Noti JD, Coyle JP, Derk RC, Blachere FM, et al. Maximizing fit for cloth and medical procedure masks to improve performance and reduce SARS-CoV-2 transmission and exposure, 2021. MMWR 2021;70:254–7.
Gena AW, Voelker C, Settles GS. Qualitative and quantitative Schlieren optical measurement of the human thermal plume. Indoor Air 2020;30:757–66.
Johnson GR, Morawska L, Ristovski ZD, Hargreaves M, Mengersen K, Chao CYH, et al. Modality of human expired aerosol size distributions. J Aerosol Sci 2011;42:839–51.
Konda A, Prakash A, Moss GA, Schmoldt M, Grant GD, Guha S. Aerosol filtration efficiency of common fabrics used in respiratory cloth masks. ACS Nano 2020;14:6339–47.
Liu Y, Roll J, Van Kooten S, Deng XY. Schlieren photography on freely flying hawkmoth. Biol Lett 2018;14.
Petersen E, Koopmans M, Go U, Hamer DH, Petrosillo N, Castelli F, et al. Comparing SARS-CoV-2 with SARS-CoV and influenza pandemics. Lancet Infect Dis 2020;20:E238–44.
Poodt PWG, Heijna MCR, Christianen PCM, van Enckevort WJP, de Grip WJ, Tsukamoto K, et al. Using gradient magnetic fields to suppress convection during crystal growth. Cryst Growth Des 2006;6:2275–80.
Simha PP, Rao PSM. Universal trends in human cough airflows at large distances. Phys Fluids 2020;32(8).
Staymates M. Flow visualization of an N95 respirator with and without an exhalation valve using Schlieren imaging and light scattering. Phys Fluids 2020;32.
Tang JW, Liebner TJ, Craven BA, Settles GS. A Schlieren optical study of the human cough with and without wearing masks for aerosol infection control. J R Soc Interface 2009;6:S727–36.
Warkentin M, Thorne RE. A general method for hyperquenching protein crystals. J Struct Funct Genomics 2007;8:141–4.
Yang SH, Lee GWM, Chen CM, Wu CC, Yu KP. The size and concentration of droplets generated by coughing in human subjects. J Aerosol Med 2007;20:484–94.
Zayas G, Chiang MC, Wong E, MacDonald F, Lange CF, Senthilselvan A, et al. Cough aerosol in healthy participants: fundamental knowledge to optimize droplet-spread infectious respiratory disease management. BMC Pulmon Med 2012;12:11 https://bmcpulmmed.biomedcentral.com/articles/10.1186/1471-2466-12-11.